ELSEVIER

Journal of Alloys and Compounds 463 (2008) 288–293

Journal of ALLOYS AND COMPOUNDS

www.elsevier.com/locate/jallcom

Thermoelectric properties of $Sn_{1-x-y}Ti_ySb_xO_2$ ceramics

Toshiki Tsubota *, Teruhisa Ohno, Norihisa Shiraishi, Yuji Miyazaki

Department of Materials Science, Faculty of Engineering, Kyushu Institute of Technology, 1-1 Sensuicho, Tobata-ku, Kitakyushu 804-8550, Japan

Received 10 January 2007; accepted 2 September 2007
Available online 6 September 2007

Abstract

Thermoelectric properties of $Sn_{1-x-y}Ti_y$ Sb_xO_2 ceramics were investigated in detail. The addition of Sb into SnO_2 matrix increased the electric conductivity, σ. The increase in the σ value should be caused by the increase in the carrier concentration. The Seebeck coefficients of all the samples were negative, which means that these samples have n-type conduction. The samples of this study have porous structure. The maximum Z value of all the samples measured in this study was $2.4 \times 10^{-5}\,K^{-1}$.

Keywords: Ceramics; Thermoelectric materials; Sintering; Electrical transport; Oxide materials

1. Introduction

Because power unit of thermoelectric generation produces electric power from temperature difference, we can convert waste heat energy to electric energy by using thermoelectric power generation. Therefore, thermoelectric power generation is one of the most promising power generations for environmental conservation. However, the conversion efficiency of conventional thermoelectric power generation is insufficient in performance. The reason for this low efficiency is the low thermoelectric property of the conventional thermoelectric materials.

The thermoelectric property of material is estimated by the value of figure of merit, Z.

$$Z = \frac{S^2\sigma}{k} \tag{1}$$

where S is Seebeck coefficient, σ is electrical conductivity, and κ is thermal conductivity. The material having higher Z value possesses higher thermoelectric performance.

In general, a lot of metal oxides are stable in air at high temperature, and are safe and inexpensive. Therefore, metal oxide materials must be one of the most promising material groups as a novel thermoelectric material. So far, some researchers have been studying the thermoelectric properties of oxide materials [1–10]. Ohtaki et al. proposed that metal oxide materials are a promising group as novel thermoelectric material for the first time [1]. Tsubota et al. reported that the Z value of $Zn_{1-x}Al_xO$ is *ca.* $0.24 \times 10^{-3}\,K^{-1}$ at 1000 °C [2,3]. This Z value is almost as same as that of β-$FeSi_2$, which is a candidate for new thermoelectric material as non-oxide material [4]. Terasaki et al. reported that the Z value of Na_xCoO_2 is *ca.* $8.0 \times 10^{-4}\,K^{-1}$ at *ca.* 900 K [5,6]. This Z value is as large as that of SiGe, which is a conventional thermoelectric material [7]. After the report of the high Z value of Na_xCoO_2, some kinds of oxides are proposed as new candidate for thermoelectric material, such as $SrTiO_3$ [8], $CaMnO_3$ [9], $Ca_3Co_4O_9$ [10] and so on. However, there is no oxide material which is applied in practical use until now. Especially, there is no report about n-type oxide materials which have high thermoelectric performance.

Tin oxide, SnO_2, is a typical conductive oxide, which is used as gas sensor [11], transparent electrode [12] and so on. The conduction type of SnO_2 is n-type. Moreover, it is known that the doping of Sb_2O_5 in SnO_2 can increase the electrical conductivity. The carrier mobility of SnO_2 is known to be as large as oxide material. In the case of the material which has simple two band structure, the Z value should increase with increasing the β value, which is called material factor.

$$\beta = 8.952\left(\frac{T}{300}\right)^{5/2}\left(\frac{m^*}{m_0}\right)^{3/2}\left(\frac{\mu}{\kappa_{ph}}\right) \tag{2}$$

* Corresponding author. Tel.: +81 93 884 3324; fax: +81 93 884 3324.
E-mail address: tsubota@che.kyutech.ac.jp (T. Tsubota).

0925-8388/$ – see front matter © 2007 Elsevier B.V. All rights reserved.
doi:10.1016/j.jallcom.2007.09.001

where T is absolute temperature, m^* is effective mass of carrier, m_0 is electron mass, μ is carrier mobility, and κ_{ph} is lattice thermal conductivity. From the formula (2), high μ value is desired to achieve high Z value.

The crystal structure of SnO_2 is rutile structure. The crystal structure of TiO_2 is also rutile structure at high temperature region. It is known that TiO_2 can dissolve into SnO_2.

Thermal conductivity, κ, of solid material is consist of

$$\kappa = \kappa_{el} + \kappa_{ph} \quad (3)$$

where κ_{el} is carrier thermal conductivity, and κ_{ph} is lattice thermal conductivity. In general, the κ_{ph} value decrease by the formation of solid solution. As shown in formulas (1) and (2), small κ value is desired to achieve high Z value.

In this study, we attempt that the doping of Sb_2O_5, which should increase the σ value, and the formation of solid solution with TiO_2, which should decrease the κ_{ph} value, in SnO_2.

2. Experimental

Fine powders of SnO_2, Sb_2O_5, TiO_2 powders were used as starting materials for this study. Samples of $Sn_{1-x-y}Ti_xSb_yO_2$ were prepared by solid state reaction. These powders were mixed in a nylon-lined ball mill for 24 h. The powder mixture was pressed into a pellet and sintered at 1300 °C for 10 h in air. The heating and cooling rate was 200 °C h^{-1}. The crystal phases in the prepared samples were determined from a powder X-ray diffraction (XRD) study using Cu Ka radiation. The electrical conductivity and Seebeck coefficients were measured simultaneously in He atmosphere up to 800 °C by ZEM-1 (ULVAC-RIKO, Inc.). The thermal conductivity was determined from the thermal diffusivity and the specific heat capacity measured by the laser flash technique (ULVAC TC-7000).

3. Results and discussion

3.1. Electrical property

3.1.1. Electrical conductivity

The temperature dependence on the electrical conductivities, σ, of $Sn_{0.99-x}Ti_xSb_{0.01}O_2$, $Sn_{1.00-y}Sb_yO_2$, and $Sn_{0.85}Ti_{0.1}Sb_{0.05}O_2$ are shown in Figs. 1 and 2. The σ values of $Sn_{0.99}Sb_{0.01}O_2$ were similar to that of $Sn_{0.95}Sb_{0.05}O_2$. Therefore, excessive addition of Sb_2O_5 is ineffective for the enhancement of the σ value. As for $Sn_{0.99-x}Ti_xSb_{0.01}O_2$, the σ value for all the samples increased with increasing temperature up to *ca.* 300 °C. In this temperature region, the σ value decreased with increasing the amount of the addition of TiO_2. Moreover, excessive addition of Sb_2O_5 was ineffective for the enhancement of the σ value when TiO_2 was added as shown in the data of $Sn_{0.85}Ti_{0.1}Sb_{0.05}O_2$. Therefore, the existence of TiO_2 must decrease the σ value. In the temperature region of above *ca.* 300 °C, the σ value for all the samples decreased with increasing temperature, except for $Sn_{0.89}Ti_{0.1}Sb_{0.01}O_2$.

3.1.2. Seebeck coefficient

The temperature dependence on the Seebeck coefficients, S, of $Sn_{0.99-x}Ti_xSb_{0.01}O_2$, and $Sn_{1.00-y}Sb_yO_2$ are shown in Figs. 3 and 4. All the S values were negative, which means that these samples have n-type conduction. The S value of SnO_2 was from −120 to −150 μV K^{-1} at all the temperature measured in this study. The absolute S value decreased with the addition of Sb_2O_5 as shown in the data of $Sn_{1-x}Sb_xO_2$ (x = 0.01, 0.05). As for $(Sn_{0.99-x}Ti_x)Sb_{0.01}O_2$, the S values for all the samples except for $Sn_{0.89}Ti_{0.1}Sb_{0.01}O_2$ were *ca.* −40 μV K^{-1} at *ca.* 50 °C, and those values were *ca.* −80 μV K^{-1} at 800 °C. The absolute S values for all the samples except for $Sn_{0.89}Ti_{0.1}Sb_{0.01}O_2$ increased with increasing temperature. The S value for the sample of $Sn_{0.89}Ti_{0.1}Sb_{0.01}O_2$ was *ca.* −140 μV K^{-1} all temperature region. The slopes for the temperature dependence of the S value for all the sample added Sb_2O_5 are almost same as shown in Figs. 3 and 4. In the case of the sample described by simple band structure, it is known that the S value depends on the value of carrier density, n. All the samples added Sb_2O_5 should have similar temperature dependences of the n values.

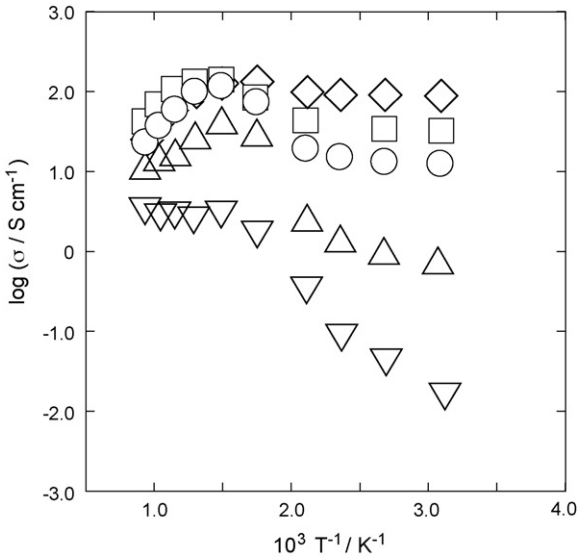

Fig. 1. Arrhenius plots of electrical conductivities of $(Sn_{0.99-x}Ti_x)Sb_{0.01}O_2$; x: ◊,0; □, 0.01; ○, 0.02; △,0.05; ▽,0.10.

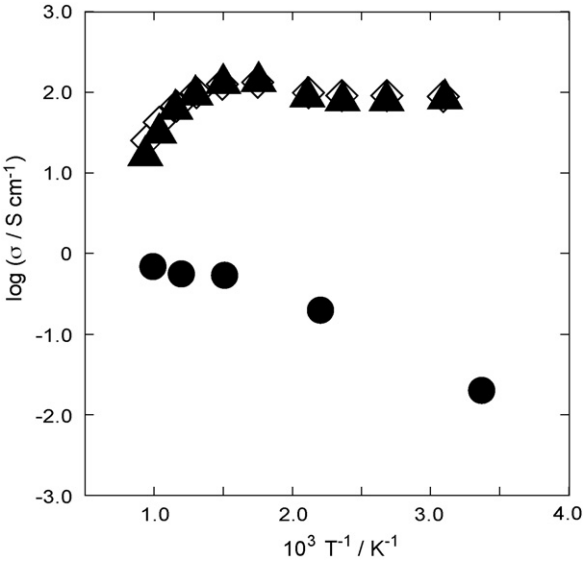

Fig. 2. Arrhenius plots of electrical conductivities of $Sn_{1.00-y}Sb_yO_2$; ◊, $Sn_{0.99}Sb_{0.01}O_2$; ▲, $Sn_{0.95}Sb_{0.05}O_2$; ●, $Sn_{0.85}Ti_{0.1}Sb_{0.05}O_2$.

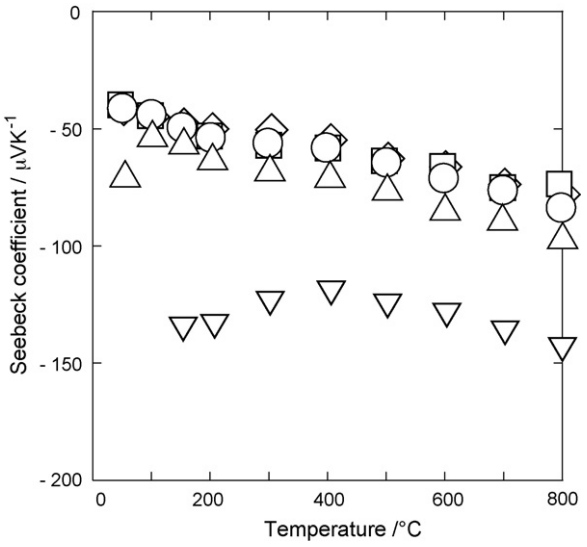

Fig. 3. Seebeck coefficients of $(Sn_{0.99-x}Ti_x)Sb_{0.01}O_2$ as a function of temperature; x: ◊, 0; □, 0.01; ◯, 0.02; △, 0.05; ▽, 0.10.

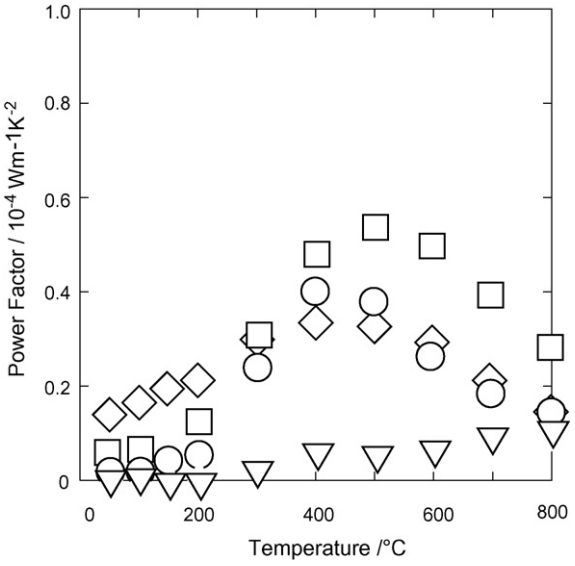

Fig. 5. Power Factor of $(Sn_{0.99-x}Ti_x)Sb_{0.01}O_2$ as a function of temperature; x: ◊, 0; □, 0.01; ◯, 0.02; △, 0.05; ▽,0.10.

3.1.3. Electrical transport property

Using Kroger-Vink notation, we can describe the mechanism of the doping with Sb_2O_5 in SnO_2.

$$Sb_2O_5 \rightarrow 2Sb_{Sn}^{\bullet} + 4O_O{}^X + 2e^- + \tfrac{1}{2}O_2 \quad (4)$$

The electrons which generate with the Sb_2O_5 solution in SnO_2 act as charge carriers. Therefore, the material has n-type conduction, and the σ value of SnO_2 increases by Sb_2O_5 doping. When TiO_2 dissolves into SnO_2, the reaction mechanism is as follows,

$$TiO_2 \rightarrow 2Ti_{Sn}{}^X + 4O_O{}^X \quad (5)$$

As shown in formula (5), no charge carrier generates with this solid solution reaction.

The electrical conductivity, σ, is consisted of

$$\sigma = ne\mu \quad (6)$$

where n is carrier density, e is charge of carrier, μ is mobility.

The Seebeck coefficient, S, for the material which has simple two band structure is describe as follows,

$$S = \pm\frac{k}{e}\left[r + 2\ln\frac{2(2\pi m^* kT)^{3/2}}{h^3 n}\right] \quad (7)$$

where k is Boltzmann constant, e is elementary charge, m^* is effective mass of charge carrier, T is absolute temperature, h is Planck's constant, and n is carrier density.

The Ti atom in SnO_2 matrix must act as the scattering center, which decreases the μ value. As shown in Fig. 1, the reduc-

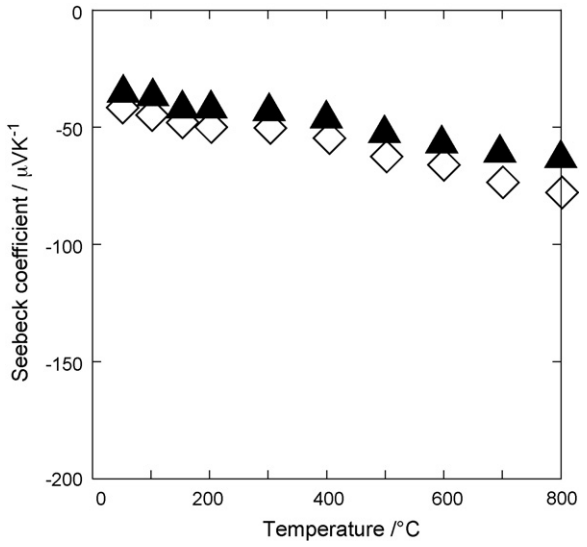

Fig. 4. Seebeck coefficients of $Sn_{1.00-x}Sb_xO_2$ as a function of temperature; ◊, $Sn_{0.99}Sb_{0.01}O_2$; ▲, $Sn_{0.95}Sb_{0.05}O_2$.

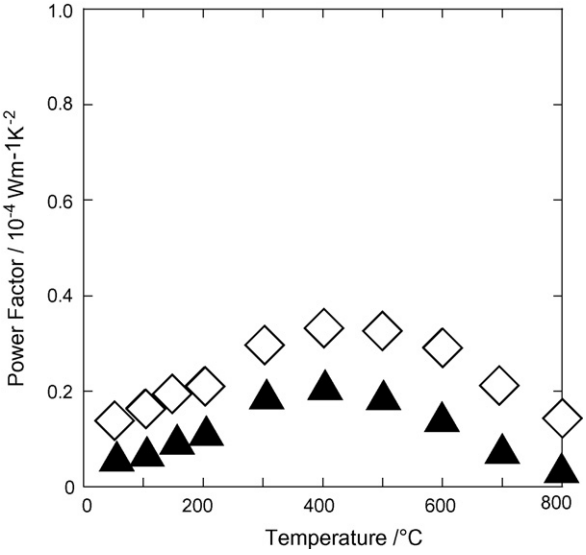

Fig. 6. Power Factor of $Sn_{1.00-x}Sb_xO_2$ as a function of temperature; ◊, $Sn_{0.99}Sb_{0.01}O_2$; ▲, $Sn_{0.95}Sb_{0.05}O_2$.

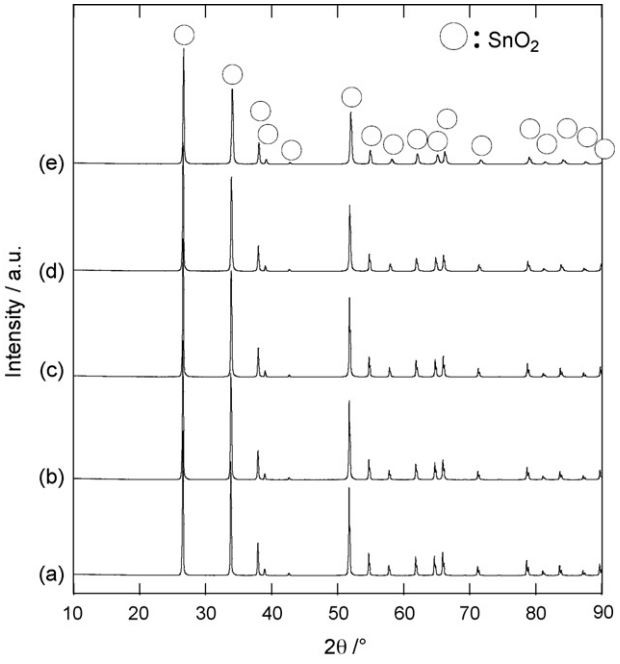

Fig. 7. Powder X-ray diffraction patterns of $(Sn_{1-x}Ti_x)Sb_{0.01}O_2$, (a) $x=0$, (b) $x=0.01$, (c) $x=0.02$, (d) $x=0.05$, (e) $x=0.10$.

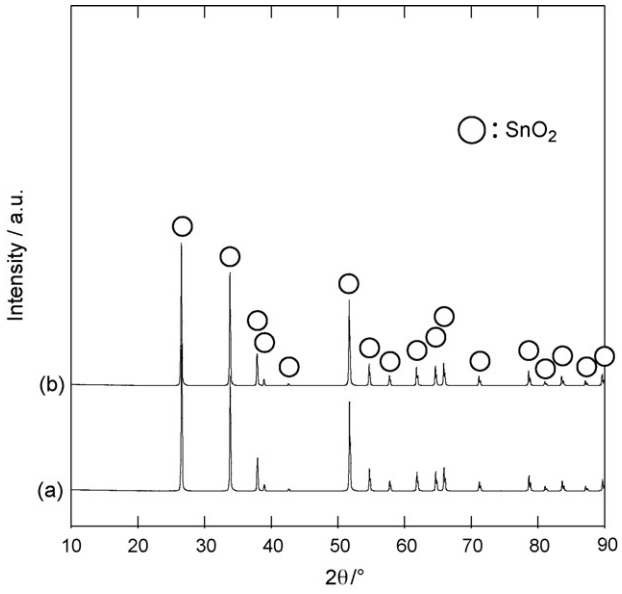

Fig. 8. Powder X-ray diffraction patterns of $Sn_{1-x-y}Ti_ySb_xO_2$, (a) $Sn_{0.9}Ti_{0.1}O_2$, (b) $Sn_{0.95}Sb_{0.05}O_2$.

tion of the μ value should result in the decrease in the σ value.

From the formula (5), we can presume that the addition of TiO_2 in SnO_2 dose not affect the carrier density of SnO_2 matrix. That is, we can presume that the addition of TiO_2 causes the reduction of the μ value and does not affect the n value. As shown in Figs. 1 and 3, the σ value decreased with increasing the amount of the addition of TiO_2, and the S value was almost independent of the amount of the addition of TiO_2. Therefore, this presumption agrees with the experimental results, except for the sample of $Sn_{0.89}Ti_{0.1}Sb_{0.01}O_2$.

3.1.4. Electrical thermoelectric property

The temperature dependence on the power factor, $S^2\sigma$, of $Sn_{1-x-y}Ti_xSb_{0.01}O_2$ are shown in Figs. 5 and 6. The $S^2\sigma$ values for these samples depended on temperature. All the samples except for $Sn_{0.89}Ti_{0.1}Sb_{0.01}O_2$ had the maximum $S^2\sigma$ value at 400–500 °C. The highest $S^2\sigma$ value of all these samples was 0.53×10^{-4} W m^{-1} K^{-2} at 500 °C. The reported $S^2\sigma$ value of

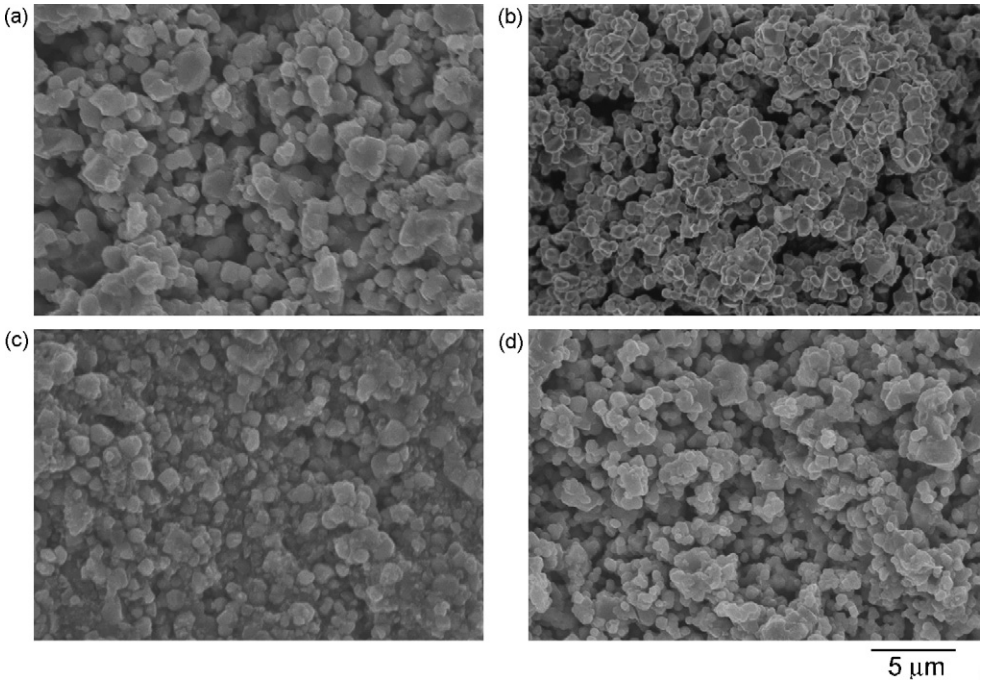

Fig. 9. SEM images of $Sn_{1-x-y}Ti_ySb_xO_2$, (a) SnO_2, (b) $Sn_{0.95}Sb_{0.05}O_2$, (c) $Sn_{0.9}Ti_{0.1}O_2$, (d) $Sn_{0.98}Ti_{0.01}Sb_{0.01}O_2$.

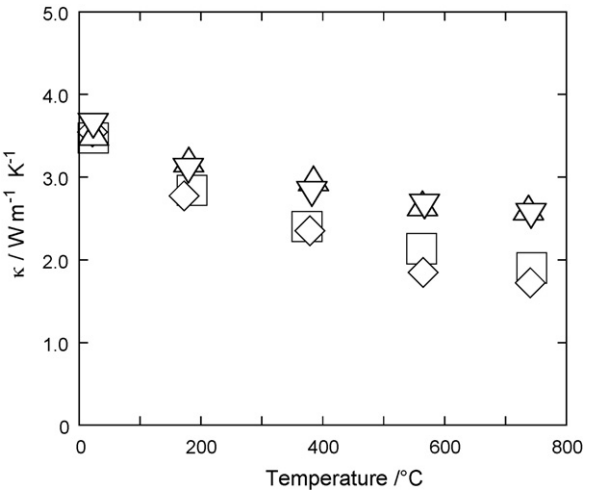

Fig. 10. Thermal conductivity of $(Sn_{0.99-x}Ti_x)Sb_{0.01}O_2$ as a function of temperature; x: ◊, 0; □, 0.01; △, 0.05; ▽, 0.10.

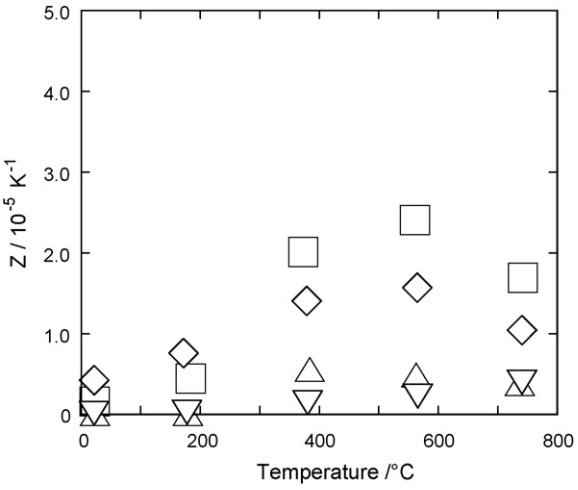

Fig. 12. Figure of merit of $(Sn_{0.99-x}Ti_x)Sb_{0.01}O_2$ as a function of temperature; x: ◊, 0; □, 0.01; △, 0.05; ▽, 0.10.

$CaMn_{0.96}Ru_{0.03}O_{3-\delta}$ system was 1.85×10^{-4} W K^{-2} m^{-1} at 1000 K [9]. The reported $S^2\sigma$ value of $Ca_3Co_4O_9$ system was 1.2×10^{-4} W K^{-2} m^{-1} at 700 °C [10]. The value for the sample of this study is smaller than those of oxides.

3.2. Crystal structure

The XRD patterns of are shown in Figs. 7 and 8. As shown in Figs. 7 and 8, all the peaks appeared in these charts were assigned to SnO_2 phase, and there is no peak assigned to TiO_2 phase or Sb_2O_5 phase. Therefore, doped Sb_2O_5 and doped TiO_2 must dissolve into SnO_2.

3.3. Micro structure

SEM images for the samples of $Sn_{1-x-y}Ti_ySb_xO_2$ are shown in Fig. 9. As shown in Fig. 9, all the samples have porous structure. All the samples consist of the grains which are 0.5–1 μm in diameters. These results should means that both TiO_2 and Sb_2O_5 cannot act as sintering agent for SnO_2. The degree of sintering for the samples cannot explain the change of the σ value with the doping of Sb_2O_5 or TiO_2.

3.4. Thermal conductivity

The temperature dependences of the thermal conductivity, κ, of $Sn_{1-x-y}Ti_ySb_xO_2$ are shown in Figs. 10 and 11. The κ values decreased with increasing temperature. All the κ values for the samples were *ca.* 3.5 W m^{-1} K^{-1} at room temperature, and these values at 800 °C were *ca.* 3–*ca.* 2 W m^{-1} K^{-1}. These κ values are small, compared with normal ceramics. The samples of this study have porous structure as shown in Fig. 9. The reason for the small κ values must be this structure.

The thermal conductivity of solid material, κ, is consists of the phonon thermal conductivity, κ_{ph}, and the carrier thermal conductivity, κ_{el}, as shown in formula (3). From Wiedemann-

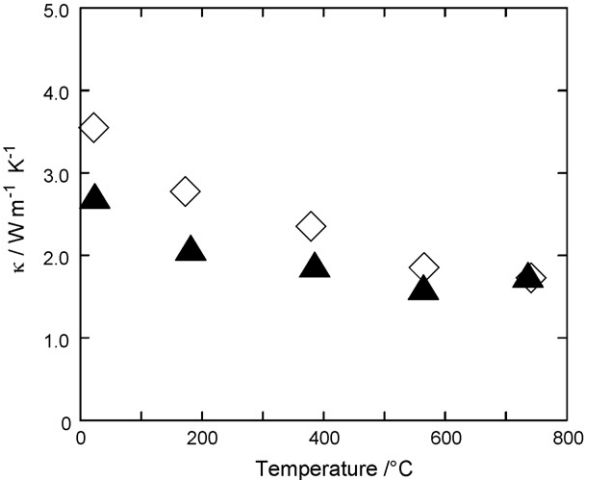

Fig. 11. Power factor of $Sn_{1-x}Sb_xO_2$ as a function of temperature; ◊, $Sn_{0.99}Sb_{0.01}O_2$; ▲, $Sn_{0.95}Sb_{0.05}O_2$.

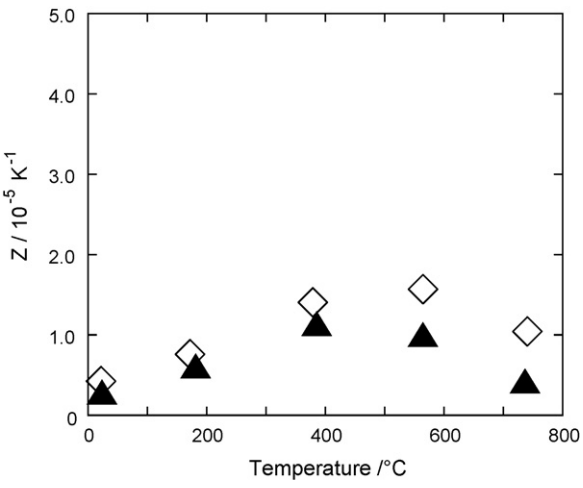

Fig. 13. Figure of merit of $Sn_{1-x}Sb_xO_2$ as a function of temperature ◊, $Sn_{0.99}Sb_{0.01}O_2$; ▲, $Sn_{0.95}Sb_{0.05}O_2$.

Frantz law, the κ_{el} value is as follows,

$$\kappa_{el} = \sigma_{LT} \quad (8)$$

where L (=2.45 × 10^{-8} W Ω K^{-2}) is Lorentz number, T is absolute temperature. Because the σ values for the samples are 10^{-2} to 2 × 10^{2} S cm^{-1} and the T value are 300–1073 K, the κ_{el} values are much smaller than the κ_{ph} values. Therefore, most part of the κ value for the samples of this study is the κ_{ph} value.

3.5. Figure of merit

The temperature dependences of the figure of merit, Z, of $Sn_{1-x-y}Ti_xSb_yO_2$ are shown in Figs. 12 and 13. The maximum Z value of all the samples measured in this study was 2.4 × 10^{-5} K^{-1}. This Z value is insufficient for the practical application. Therefore, we must perform other approaches for the enhancement of the Z value for the material.

4. Conclusions

The thermoelectric properties of $Sn_{1-x-y}Ti_xSb_yO_2$ were measured in this study. The Seebeck coefficients of all the samples were negative, which means that all the samples had *n* type conduction. All the samples had porous structure. This structure must be the reason for the small thermal conductivities.

Acknowledgements

The authors thank to Mr. Mamoru Minami and Mr. Kenji Yoshimura of Fukuoka Industrial Technology Center for their kind cooperation on the laser flash measurement of κ.

References

[1] M. Ohtaki, D. Ogura, K. Eguchi, H. Arai, J. Mater. Chem. 4 (1994) 653.
[2] M. Ohtaki, T. Tsubtoa, K. Eguchi, H. Arai, J. Appl. Phys. 79 (1996) 1816.
[3] T. Tsubota, M. Ohtaki, K. Eguchi, H. Arai, J. Mater. Chem. 7 (1997) 85.
[4] M. Ito, T. Tada, S. Hara, J. Alloy Compd. 9 (2006) 408.
[5] I. Terasaki, Y. Sasago, K. Uchinokura, Phys. Rev. B 56 (1997) 12685.
[6] M. Ito, T. Nagira, D. Furumoto, S. Katsuyama, H. Nagai, Scrip. Mater. 48 (2003) 403.
[7] M.S. El-Genk, H.H. Saber, Energy Convers. Manage. 46 (2005) 1083.
[8] H. Muta, K. Kurosaki, S. Yamanaka, J. Alloy Comp. 368 (2004) 22.
[9] Y. Zhou, I. Matsubara, R. Funahashi, G. Xu, M. Shikano, Mater. Res. Bull. 38 (2003) 341.
[10] S. Li, R. Funahashi, I. Matsubara, H. Yamada, K. Ueno, S. Sodeoka, Ceram. Int. 27 (2001) 321.
[11] L. Gajdosik, Sens. Actuators B 106 (2005) 691.
[12] M. Okuya, S. Kaneko, K. Hiroshima, I. Yagi, K. Murakami, J. Eur. Ceram. Soc. 21 (2001) 2099.